

## Reliability Assessment of Light-Emitting Diode Packages with Both Luminous Flux Response Surface Model and Spectral Power Distribution Method

Chen, Wei; Fan, Jiajie; Qian, Cheng; Pu, Bin; Fan, Xuejun; Zhang, Guo Qi

**DOI**

[10.1109/ACCESS.2019.2916878](https://doi.org/10.1109/ACCESS.2019.2916878)

**Publication date**

2019

**Document Version**

Final published version

**Published in**

IEEE Access

**Citation (APA)**

Chen, W., Fan, J., Qian, C., Pu, B., Fan, X., & Zhang, G. Q. (2019). Reliability Assessment of Light-Emitting Diode Packages with Both Luminous Flux Response Surface Model and Spectral Power Distribution Method. *IEEE Access*, 7, 68495-68502. Article 8715353. <https://doi.org/10.1109/ACCESS.2019.2916878>

**Important note**

To cite this publication, please use the final published version (if applicable). Please check the document version above.

**Copyright**

Other than for strictly personal use, it is not permitted to download, forward or distribute the text or part of it, without the consent of the author(s) and/or copyright holder(s), unless the work is under an open content license such as Creative Commons.

**Takedown policy**

Please contact us and provide details if you believe this document breaches copyrights. We will remove access to the work immediately and investigate your claim.

Received April 6, 2019, accepted May 3, 2019, date of publication May 15, 2019, date of current version June 6, 2019.

Digital Object Identifier 10.1109/ACCESS.2019.2916878

# Reliability Assessment of Light-Emitting Diode Packages With Both Luminous Flux Response Surface Model and Spectral Power Distribution Method

WEI CHEN<sup>1,2</sup>, JIAJIE FAN<sup>1,2,3</sup>, (Senior Member, IEEE), CHENG QIAN<sup>1,4</sup>, (Member, IEEE), BIN PU<sup>2</sup>, XUEJUN FAN<sup>5</sup>, (Fellow, IEEE), AND GUOQI ZHANG<sup>3</sup>, (Fellow, IEEE)

<sup>1</sup>College of Mechanical and Electrical Engineering, Hohai University, Changzhou 213022, China

<sup>2</sup>Changzhou Institute of Technology Research for Solid State Lighting, Changzhou 213161, China

<sup>3</sup>Department of Microelectronics, EEMCS Faculty, Delft University of Technology, Delft 2628, The Netherlands

<sup>4</sup>School of Reliability and Systems Engineering, Beihang University, Beijing 100083, China

<sup>5</sup>Department of Mechanical Engineering, Lamar University, Beaumont, TX 77710, USA

Corresponding author: Jiajie Fan (jay.fan@connect.polyu.hk)

This work was supported in part by the National Key Research and Development Program of China under Grant 2017YFB0403500, in part by the National Natural Science Foundation of China under Grant 51805147 and Grant 61673037, in part by the Six Talent Peaks Project in Jiangsu Province under Grant GDZB-017, in part by the Fundamental Research Funds for the Central Universities under Grant 2017B15014 and Grant 2018B792X14, and in part by the Postgraduate Research and Practice Innovation Program of Jiangsu Province under Grant SJCX18\_0207.

**ABSTRACT** The inherent luminous characteristics and stability of LED packages during the operation period are highly dependent on their junction temperatures and driving currents. In this paper, the luminous flux of LED packages operated under a wide range of driving currents and junction temperatures are investigated to develop a luminous flux response surface model. The coefficients of the proposed model are further extracted to compare the luminous efficacy decay mechanisms of LED packages with different packaging structures. Furthermore, a spectral power distribution (SPD) method modeled by the Gaussian function is proposed to analyze the long-term degradation mechanisms of all selected LED packages. The results of this study show that: (1) The luminous flux of phosphor converted white LED decreases to accompany with the increase of junction temperature, while that of bare blue LED die keeps relatively stable; (2) The proposed general luminous flux response surface model can be used to predict the luminous flux of LEDs with different packaging technologies accurately, and it can be known from the proposed model that the influences of driving current and temperature on LED chip and phosphor vary with different packaging structures; and (3) The driving current and temperature dependent sensitivities and degradation mechanisms of LED packages can be investigated by using both the luminous flux response surface model and the spectral power distribution method.

**INDEX TERMS** Light-emitting diode, luminous flux response surface model, spectral power distribution, luminous efficacy decay, degradation mechanism.

## I. INTRODUCTION

The first visible light emitted diode (LED) was discovered in 1962 [1] and a blue LED chip with high efficiency was invented in 1990s, thereafter LED has made great progress in lighting industry [2]–[5]. About 19% of electricity is consumed for lighting around the world [6],

The associate editor coordinating the review of this manuscript and approving it for publication was Bo Sun.

LED has been regarded with great potential for electricity saving as its higher luminous efficacy [7]. Moreover, it also benefits with high efficiency, high reliability, long lifespan, high-speed response and small volume. With the development of LED technology, high power LED packages are increasingly applied to many lighting and beyond-lighting industries, i.e. automotive lighting [8], indoor plant cultivation [9], healthcare [10], data communication [11], [12] and so on.

However, despite these excellent properties, there is a big shackle called “efficiency/efficacy droop” to restrict on LED’s application [13]. Several previous research works have manifested that high junction temperature ( $T_j$ ) and high driving current ( $I_f$ ) can cause a significant droop on the luminous efficacy of most LEDs [14]–[18]. With the temperature raising, the internal quantum efficiency of LED chip will decrease because of the temperature dependence of radiation recombination and Auger recombination [19]. The Auger recombination is a non-radiation recombination which does harm to the luminous efficacy. Sukhoivanov *et al.* [20] found that the Auger recombination rate was exponentially depended on the temperature. Other studies [21], [22] have proved that the Auger recombination was the major mechanism of efficiency droop and it could be reinforced when the driving current increases. There are also several other reasons for the efficiency droop and many studies have been forwarded to explain the efficiency droop by using the defect-assisted mechanisms, spontaneous emission reduction, carrier injection mechanisms [23] and carrier leakage model [24]–[26]. Moreover, different semi-polar planes, thickness of Quantum-Well (QW) and threading dislocation density also had impacts on the efficiency droop of LEDs [27]–[31]. Kim *et al.* [32] found that the efficiency droop might not related to the junction temperature under high injection conditions, rather it was related to the recombination of carriers outside the MQW region. In the package level, phosphor converted white LED (pc-WLED) package is widely used as one of cost-effective light sources, which is always composed by the blue LED chip, phosphors and other packaging materials. Thus, the efficiency droop in LED package level will consider the transient stability and long-term reliability of all above components. However, there is still no appropriate method to model the luminous efficacy decay of LED package.

To understand the luminous efficacy decay mechanism of LED in package level and its long-term degradation mechanism, two experiments are firstly designed in this study for LED packages with four general packaging structures, those are the transient thermal and luminous characteristics measurements and accelerated ageing test. In our previous study [33], a universal luminous flux response surface model was developed to relate the luminous flux with junction temperature and driving current effectively. Therefore, the luminous flux response surface model considering the electric-thermal-luminous coupling effect and the Gaussian based SPD model are proposed in this paper to predict the LED package level luminous efficacy decay and long-term degradation mechanisms respectively.

The remaining of this paper is organized as follows: Section II proposes the luminous flux response surface model and spectral power distribution method. Section III introduces the test samples and experimental setups used in this study. Section IV discusses the effect of different packaging structures on the efficiency droop mechanism and degradation mechanism based on the experiment results, the proposed

luminous flux response surface model and Gaussian based SPD model. Finally, the concluding remarks are presented in section V.

## II. THEORIES AND METHODOLOGIES

### A. LUMINOUS FLUX RESPONSE SURFACE MODEL

The increase of junction temperature and driving current can deteriorate the luminous efficacy of LEDs. Thus, to predict the luminous flux of LED under different operation conditions, a general luminous flux response surface model [33] is proposed as shown in Eq. (1) (hereby named *Model 1*):

$$\phi_v(I_f, T_j) = \phi_{v0} \left( \frac{I_f}{I_{f0}} \right)^D e^{\ln(HC) \left( \frac{T_j - T_{j0}}{75} \right)} \quad (1)$$

where  $HC$ ,  $D$ ,  $T_{j0}$ , and  $I_{f0}$  correspond to the *Hot-Cold (HC)* factor, droop constant, rated operating temperature and rated driving current, respectively.  $HC$  and  $D$  represent the degree of luminous efficacy droop with the increase of the junction temperature and driving current, respectively.  $\phi_{v0}$  is the luminous flux of the LED at  $T_{j0}$  and  $I_{f0}$ .

With the development of LED’s technology and the expansion of applied fields, Eq. (1) has often been used to predict the luminous flux of high-power LED under different operating conditions. However, the *Model 1* is not always applicable, particularly in extremely harsh conditions, such as the too high or too low driving current. To fix this problem, a modification of *Model 1* is proposed as shown in Eq. (2) (hereby named *Model 2*):

$$\phi_v(I_f, T_j) = \phi_{v0} \left( \frac{I_f}{I_{f0}} \right)^{\left( D + C_e \ln \left( \frac{I_f}{I_{f0}} \right) \right)} \left( \alpha_1 - \alpha_2 n \left( \frac{T_j - T_{j0}}{100 - T_{j0}} \right) \right) \quad (2)$$

Furtherly, the  $\alpha_1$  and  $\alpha_2$  can be obtained from the fellow equations:

$$\alpha_1 = 1 + \alpha_2 \quad (3)$$

$$\alpha_2 = \frac{HC(I_f) - 1}{1 - n} \quad (4)$$

$$\alpha_3 = \left( \frac{m + I_f}{I_{f0}} \right) \quad (5)$$

$$HC(I_f) = HC_0 \cdot \alpha_3 \cdot \left( \frac{I_f}{m + I_f} \right) \quad (6)$$

in Eq. (2),  $HC_0$ ,  $C_e$ ,  $m$ ,  $n$  represents the Hot Cold factor for rated driving current, nonlinearity droop coefficient, current coefficient of  $HC$  factor, temperature power coefficient for flux, respectively. The part of  $C_e * \ln(I_f * I_{f0}^{-1})$  is added to improve prediction accuracy of the model at an extremely low or high driving current condition.

### B. SPECTRAL POWER DISTRIBUTION METHOD

The SPD of widely used pc-WLED always has multiple peaks: one located in the short wavelength region represents the blue light emitted by LED chip, the others are located in the long wavelength region with converted light from

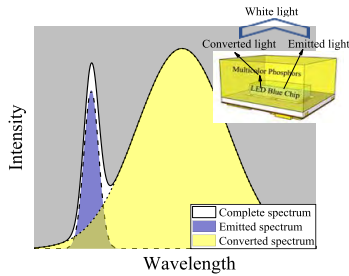


FIGURE 1. The structure and light principle of pc-WLED and their SPD.

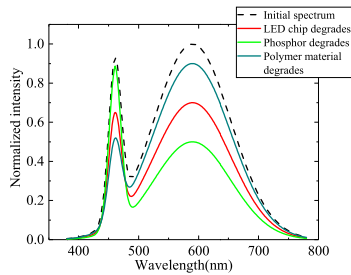


FIGURE 2. Different failure modes occurred in a pc-WLED.

phosphors, as shown in Fig. 1. Failure modes can be found by using the area of the spectrum which represent the radiant power of the LED.

According to our previous studies [34], the failure modes of pc-WLEDs can be classified as three sections: as shown in Fig. 2, (1) chip degradation may show the proportional decrease of the areas of both the emitted spectrum and the converted spectrum, for the reason that the lumen of phosphor depends on the energy of the emitted blue light; (2) phosphors degradation could result in the more decrease of the area of the converted spectrum; (3) encapsulation silicone degradation will indicate the more decrease of the area of the emitted spectrum, for the reason that the silicone is always sensitive to short wavelength light. In general, these three failure modes always appear jointly in an LED during the ageing process.

In order to acquire the areas of blue light emitting spectrum and the phosphor-converted spectrum, it is convenient to use the Gaussian model to fit the entire spectrum and to extract the features of spectrum. Then the entire SPD of the pc-WLED is expressed as:

$$y = y_0 + \frac{a_1}{w_1 \sqrt{\frac{\pi}{2}}} e^{-2\left(\frac{x-x_{c1}}{w_1}\right)^2} + \frac{a_2}{w_2 \sqrt{\frac{\pi}{2}}} e^{-2\left(\frac{x-x_{c2}}{w_2}\right)^2} \quad (7)$$

in which  $y_0$  is the baseline offset,  $a_1$ ,  $x_{c1}$ , and  $w_1$  are the area, peak wavelength and full width at half maxima of the emitted blue light spectrum, respectively; and  $a_2$ ,  $x_{c2}$ , and  $w_1$  are the area, peak wavelength and full width at half maxima of the converted light spectrum, respectively.

### III. SAMPLES AND EXPERIMENTS

In this section, the test samples used in this study are introduced firstly. Then, two experimental setups, including

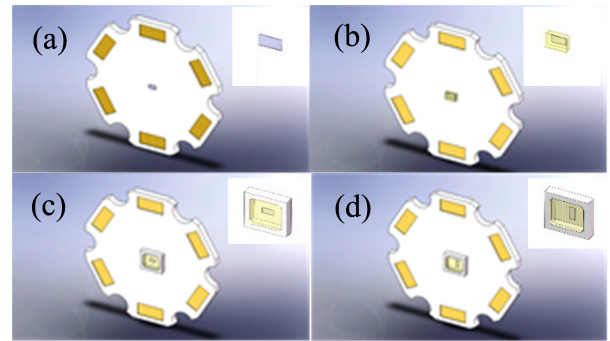


FIGURE 3. Schematic diagram of test samples: (a) CF2040 blue LED; (b) CF2040 white LED; (c) HL mid-power 3000K white LED; (d) HL mid-power 6000K white LED.

the junction temperature and luminous flux measurements under different driving currents and case temperatures, and a step-stress accelerated thermal ageing test (SSATAT) are designed.

#### A. TEST SAMPLES

There are four kinds of LED packages with two common packaging technologies used in this study, those are marked as the CF2040 blue LED and the CF2040 white LED with the flip-chip packaging, the HL mid-power 3000K white LED and HL mid-power 6000K white LED with the wire-bonding packaging. The schematic packaging structures of all test samples are shown in Fig. 3. To be compared, although both CF2040 blue LED and CF2040 white LED are with the same type of LED chip, the CF2040 white LED is covered by a phosphor/silicone composite working as a light-converter and chip-protector. The HL mid-power 3000K white LED and HL mid-power 6000K white LED are with the same type of LED chip, but they are with different phosphors. The rated currents of CF2040 blue and white LEDs are 200mA and the rated currents of two HL mid-power white LEDs are 60mA. As described in TABLE 1, among all kinds of LEDs, HL mid-power 3000K and 6000K white LEDs will undergo an SSATAT test, so their test sample IDs are marked as #5 and #6 respectively. The quantity of each sample is shown in TABLE 1. The averaged measured parameters of all samples are used in this study for analysis.

#### B. EXPERIMENTS

TABLE 2 lists the test schemes of all samples under different driving currents and different case temperatures. The specific experimental process is shown in Fig. 4. It indicates that the purpose of experiments in this work is to quantitatively build the relationship between the optical parameters, such as luminous flux and luminous efficacy, with the driving current and junction temperature. In all experiments, the constant current (CC) was adopted to power-on the test samples.

##### 1) JUNCTION TEMPERATURE MEASUREMENT

In this experiment, the junction temperatures of test samples treated under different conditions were measured by the

TABLE 1. Brief description of the test samples.

Test sample IDs	Brief description	Sample quantity
#1	Bare blue LED chip (Chip type: CF2040)	5
#2	White LED chip (Chip type: CF2040)	5
#3	HL mid-power 3000K white LED	15
#4	HL mid-power 6000K white LED	15
#5	HL mid-power 3000K white LED undergoes accelerated test	15
#6	HL mid-power 6000K white LED undergoes accelerated test	15

TABLE 2. Test schemes for all test samples.

Samples	Test scheme
#1,#2 $I_f=200\text{mA}$	<b>Driving currents:</b> from 50mA to 650mA with an increment of 25 mA
	<b>Case temperatures:</b> from 30°C to 90°C in an increment of 10°C
#3,#4,#5,#6 $I_f=60\text{mA}$	<b>Driving currents:</b> from 20mA to 160mA in an increment of 20 mA
	<b>Case temperatures:</b> from 30°C to 90°C in an increment of 10°C

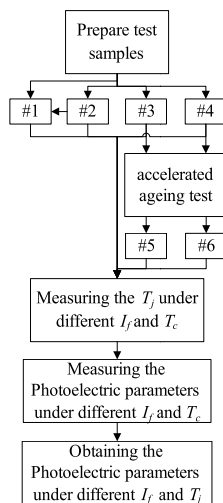


FIGURE 4. The flow chart of experiments.

junction temperature measurement instrument (Model: LEETS LEDT-300B with the accuracy of  $T_j \pm 1^\circ\text{C}$ , the accuracy of  $K$  coefficient  $\pm 0.5^\circ\text{C}$ ). The junction temperature measurement was performed based on the forward voltage method [35].

The experimental setup is shown in Fig.5, which consists of a LEETS LEDT-300B instrument, a thermal chamber (Model: ESPEC ST-110), a DC power supply (Model: KEYSIGHT N5751), a thermal control platform and a data

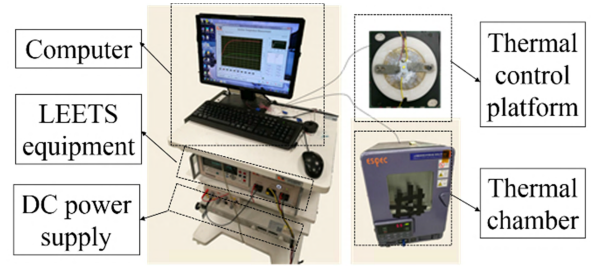


FIGURE 5. The junction temperature measurement experimental setup.

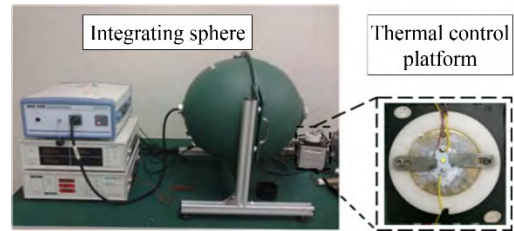


FIGURE 6. The photoelectric parameter measurement system.

acquisition computer. The thermal chamber is used to control the environment temperature for the purpose of calibrating the  $K$  coefficient of each test sample. The thermal control platform is applied to control the substrate temperature of test sample.

2) PHOTOELECTRIC PARAMETERS MEASUREMENT

In this part, the photoelectric parameters in thermal equilibrium state of all test samples were measured based on the equipment setup shown in Fig.6. It has an integrating sphere (Model: EVERFINE HASS2000), a DC power supply (Model: KEYSIGHT N5751), a thermal control platform system, and a data acquisition computer. The test samples were fixed on the thermal control platform by using heat dissipation paste, and then placed in the integrating sphere for the photoelectric parameter measurement. Five minutes after lighting, all test samples reach to the thermal equilibrium state.

3) ACCELERATED AGEING TEST

To investigate the long-term degradation mechanisms of white LEDs, a SSATAT was designed for two HL mid-power white LEDs driven by a rated constant current 60mA. The prepared samples were divided into two groups, Group A (3000K, sample #5) and Group B (6000K, sample #6). The experimental setup is shown in Fig. 7. The step-stress temperature is set from 55°C to 95°C with an increment of 10°C in every 504 hours.

IV. RESULTS AND DISCUSSIONS

A. EXPERIMENTAL RESULTS AND ANALYSIS

The junction temperatures measurement results for the six samples are shown in Fig. 8. As shown in Fig. 8(a), the junction temperatures of sample #2 are mostly higher than those



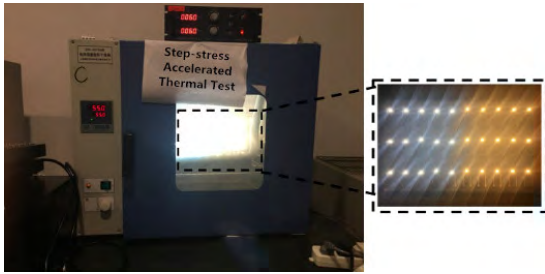


FIGURE 7. The step-stress accelerated thermal ageing test setup.

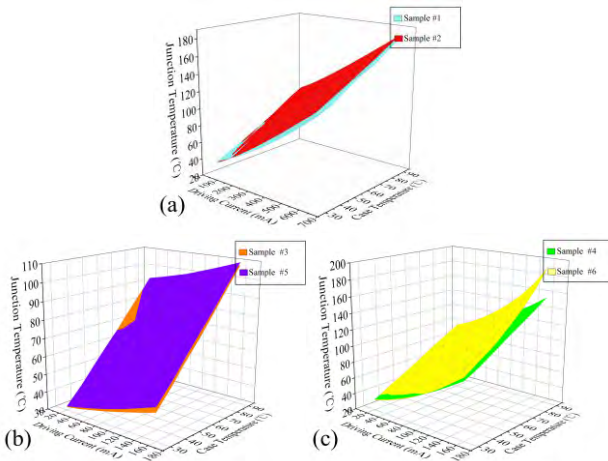


FIGURE 8. The junction temperature response surfaces of test samples under different conditions of driving current and case temperature: (a) sample #1 and #2; (b) sample #3 and #5; (c) sample #4 and #6.

of sample #1 under most conditions, because of the effect of phosphor self-heating [36] occurred in sample #2. Beyond that, silicone material used in sample #2 also can make negative influence on heat dissipation. LEDs convert electrical energy into both optical energy and thermal energy. If the luminous efficiency of LED was degraded, more heat will be produced, which leads to the increase of junction temperature. As shown in Fig. 8(b) and (c), the junction temperatures of sample #5 and #6 are higher than those of sample #3 and #4, respectively, which indicates that both sample #3 and sample #4 have degraded, after the ageing test.

Fig. 9. plots the luminous flux of test samples under different driving currents and junction temperatures, the slopes are shown in TABLE 3 and TABLE 4. As a light-conversion of phosphors, it is can be known that the luminous flux of sample #2 is much high than that of sample #1, shown in Fig. 9(a) and (b). As shown in Fig. 9(a), there is a slight improve of luminous flux for sample #1 with the increase of junction temperature. Red-shift occurs in the spectrum of sample #1 with the increase of temperature, which leads to a higher spectral luminous efficacy. As shown in Fig. 9(c) to (f), the luminous flux of sample #5 and #6 are lower than sample #3 and #4, respectively, which also indicates that sample #3 and sample #4 all have degraded, after aging. As shown in TABLE 3 and TABLE 4, the slopes of all samples decrease

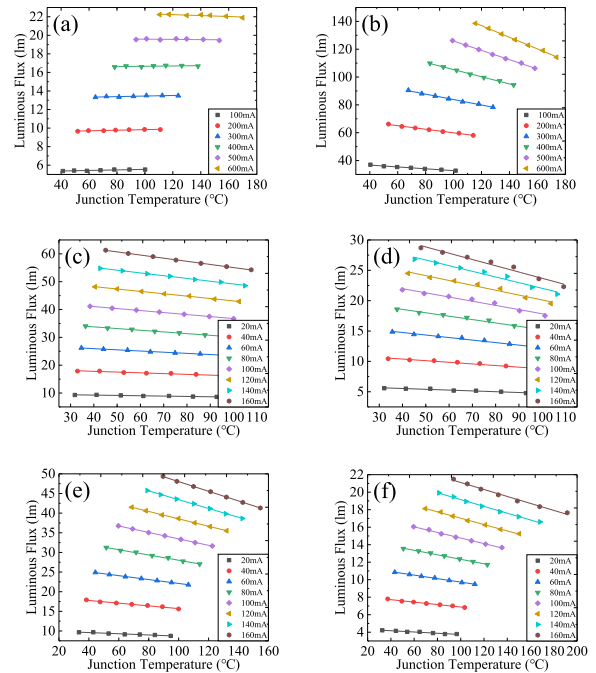


FIGURE 9. The luminous flux measurement results of the of test samples under different conditions of driving current and junction temperature: (a) sample #1; (b) sample #2; (c) sample #3; (d) sample #5; (e) sample #4; (f) sample #6.

TABLE 3. The slopes of sample #1 and sample #2.

Sample	100 mA	100 mA	100 mA	100 mA	100 mA	100 mA
#1	0.0029	0.0032	0.0030	0.0018	-0.0012	-0.0052
#2	-0.0667	-0.1290	-0.2750	-0.3338	-0.3689	-0.4168

TABLE 4. The slopes of sample #3, sample #4, sample #5 and sample #6.

Sample	20 mA	40 mA	60 mA	80 mA	100 mA	120 mA	140 mA	160 mA
#3	0.0	0.02	0.04	0.06	0.07	0.08	0.09	0.11
#4	0.0	0.03	0.04	0.06	0.08	0.09	0.11	0.12
#5	0.0	0.02	0.04	0.05	0.06	0.08	0.09	0.10
#6	0.0	0.01	0.02	0.02	0.03	0.03	0.03	0.03

with the increase of driving current, indicating that overdriving may make LEDs more sensitive to junction temperature.

Fig.10 reveals the luminous efficacy of the six samples under the different driving currents and junction temperatures. The increase of the junction temperatures and driving currents leads to the luminous efficacy drop of all test samples except for the sample #1. It is also observed that the influences of these two loading factors on the lumen depreciation are different. Except for the blue LED samples, the luminous flux of test samples decreases more dramatically with the

TABLE 5. The fitting results by using model 1.

Sample	$D$	$HC_0$	$R^2$
#1	0.7710	0.9940	0.99842
#2	0.8345	0.8097	0.99711
#3	0.8905	0.8686	0.99975
#4	0.8189	0.8289	0.99891
#5	0.8804	0.8709	0.99946
#6	0.8178	0.8501	0.99918

TABLE 6. The fitting results by using model 2.

Sample	$D$	$C_e$	$HC_0$	$n$	$m$	$R^2$
#1	0.8167	-0.0485	1.0169	2.0554	-5.7750	0.99989
#2	0.8534	-0.0469	0.9074	1.1543	-1.7480	0.99986
#3	0.9139	-0.0295	0.8916	1.0564	-0.9219	0.99998
#4	0.8384	-0.0388	0.8890	1.0710	-0.8956	0.99996
#5	0.9097	-0.0384	0.8997	1.3839	-1.5845	0.99996
#6	0.8486	-0.0399	0.8953	0.8585	-1.2756	0.99989

increase of driving current than those with the increase of junction temperature.

**B. LUMINOUS EFFICACY DECAY MECHANISM ANALYSIS**

In this part, the *Model 1* and *Model 2* are used to fit the data collected from section A, respectively. The model coefficients of these two models are extracted by the nonlinear fitting with the 1stOpt software, and listed in TABLE 5 and TABLE 6, respectively.

The  $R^2$  value is usually used to characterize the fitting accuracy of model predictions, calculated by using the follow equation:

$$R^2 = 1 - \frac{\sum (y - \hat{y})^2}{\sum (y - \bar{y})^2} \quad (8)$$

It can be seen that both  $R^2$  values of *Model 1* and *Model 2* are close to 1, which indicates that *Model 1* and *Model 2* all have high prediction accuracy to capture the flux behavior.

A high  $D$  value (close to 1) indicates that the luminous flux of the LED is nearly proportional to its driving current. As shown in TABLE 6, the  $D$  value of sample #1(bare blue LED die) is the smallest among all test sample, so it means that an increase of applied driving current will lead to a most serious luminous efficacy droop, as shown in Fig. 10(b). This phenomenon is alleviated in the white LED package, since high driving current, which means high input power density, can also improve the light-conversion efficiency of phosphor.

As shown in the TABLE 6,  $HC_0$  of all test samples are usually less than 1, except for the blue LED (sample #1). This means that the luminous flux of the sample #1 increases a little by the increase of the junction temperature, as shown in Fig. 9(a). By contrast, the luminous fluxes of other white LED samples will decrease more serious by the increase of junction temperatures, as shown in Fig. 9(b) to (f). This may attribute to the reason that when the temperature rises, the efficiency drop of phosphors can accelerate the lumen depreciation of LED chip.

TABLE 7. The results of fitting using Gaussian model.

Sample	$a_1$	$a_2$	$R^2$
#3	0.00720	0.06884	0.99011
#5	0.00517	0.03914	0.99067
Reduction rate / %	28.19	43.14	/
#4	0.01564	0.06218	0.99460
#6	0.01363	0.02870	0.99374
Reduction ratio / %	12.85	53.84	/

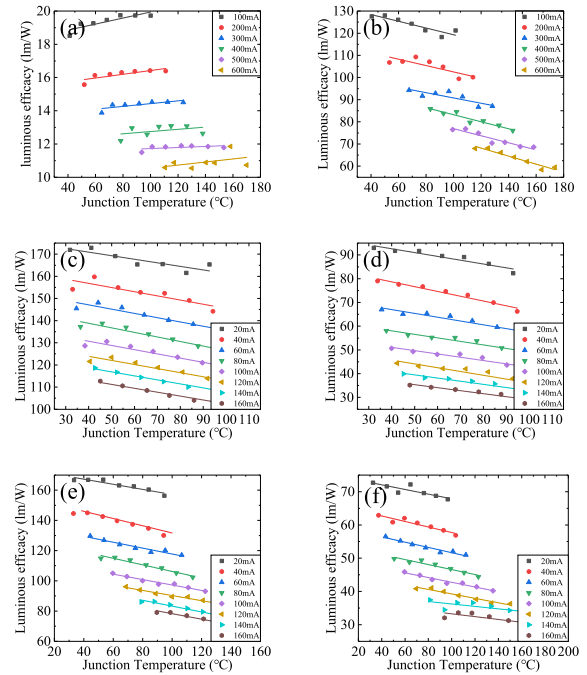
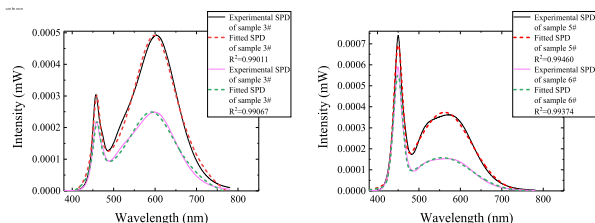


FIGURE 10. The results of the luminous efficacy under different driving current and different junction temperature: (a) sample #1; (b) sample #2; (c) sample #3; (d) sample #5; (e) sample #4; (f) sample #6.

**C. LONG-TERM LUMEN DEGRADATION MECHANISM ANALYSIS**

The mid-power 3000K and 6000K white LEDs are selected to study the degradation mechanism of white LEDs aged under SSATAT. The SPD data were collected from the integrating sphere. Fig. 11 shows the fitting results, in which the fitted SPDs with the proposed Gaussian based model, as shown in Eq. (7), agree well with experimental data ( $R^2$  is high than 0.99). The parameters  $a_1$  and  $a_2$  are extracted and given in TABLE 7. The reduction ratio is defined as the reduced percentage of area  $a$  before and after aging.

Significant reduction rates on  $a_1$  and  $a_2$  are observed as shown in Table 7. This implies that mid-power 3000K and 6000K white LEDs all have degraded. Moreover, according to the results from all samples shown in Table 7, the reduction rate on  $a_2$  is much higher than that on  $a_1$ , probably indicating that both the LED chip degradation and the phosphors degradation have occurred in mid-power 3000K and 6000K white LEDs. The difference between the reduction rate on  $a_2$  and  $a_1$ , the reduction rate on  $a_2$  minus the reduction rate



**FIGURE 11.** The experiment and fitted SPD of mid-power 3000K and 6000K white LEDs.

on  $a_1$ , is not more than the reduction rate on  $a_1$ , hence LED chip degradation is the dominant failure mode for mid-power 3000K white LEDs. In the same way, it can be known that phosphor degradation is the dominant failure mode for mid-power 6000K white LEDs. Moreover, as shown in TABLE 6, the  $D$  value of mid-power 3000K white LED decreased after ageing, however, that of mid-power 6000K white LED increased. This indicates that LED chip degradation will result in the LED package more sensitive to driving current, but phosphor degradation can cause it less sensitive to driving current. The  $HC_0$  of both mid-power 3000K and 6000K white LEDs are increased, indicating that both chip and phosphor degradations can make white LED package less sensitive to temperature.

## V. CONCLUSIONS

In this paper, the junction temperatures and luminous flux of different LED packages operated under different driving current and case temperature conditions are firstly collected to establish the luminous flux response surface model. Both the luminous flux response surface model and SPD method are then used to assess the reliability of LED packages. The results show that: (1) The luminous flux and luminous efficacy of white LED packages decrease with the increase of junction temperature, however, the luminous flux of flip-chip bare blue LED die increases slightly under high junction temperature, as its luminous efficacy rises; (2) The proposed luminous flux response surface model can accurately describe the luminous flux as a function of junction temperature and driving current, and the extracted model coefficients reveal that driving current and temperature mainly determine the luminous efficacy decay mechanism of LED chip and phosphor respectively; (3) The degradation mechanism analysis with SPD method indicates that both degradations of LED chip and phosphor can occur in the selected mid-power white LEDs aged under the designed test condition, however, chip and phosphor degradations dominate the failure mode of 3000K and 6000K white LEDs respectively. The luminous flux response surface model fitting results show that both chip and phosphor degradations can make white LED package less sensitive to temperature, but the driving current dependent sensitivity of white LED package with aged chip is higher than that with aged phosphor.

## REFERENCES

[1] G. B. Nair and S. J. Dhoble, "A perspective perception on the applications of light-emitting diodes," *Luminescence*, vol. 30, no. 8, pp. 1167–1175, Dec. 2016.

[2] S. Dai, C.-B. Siao, S.-R. Chung, K.-W. Wang, and X. Pan, "Developed one-pot synthesis of dual-color CdSe quantum dots for white light-emitting diode application," *J. Mater. Chem. C*, vol. 6, no. 12, pp. 3089–3096, 2018.

[3] M. Anandan, "Progress of LED backlights for LCDs," *J. Soc. Inf. Display*, vol. 16, no. 2, pp. 287–310, Feb. 2008.

[4] X. Zhang, J. Zhang, Z. Dong, J. Shi, and M. Gong, "Concentration quenching of  $\text{Eu}^{2+}$  in a thermal-stable yellow phosphor  $\text{Ca}_2\text{BO}_3\text{Cl}:\text{Eu}^{2+}$  for LED application," *J. Lumin.*, vol. 132, no. 4, pp. 914–918, Apr. 2012.

[5] Z. Wang, C. Yu, W.-D. Zhong, J. Chen, and W. Chen, "Performance of a novel LED lamp arrangement to reduce SNR fluctuation for multi-user visible light communication systems," *Opt. Express*, vol. 20, no. 4, pp. 4564–4573, 2012.

[6] *Light's Labour's Lost: Policies for Energy-Efficient Lighting*, I. E. Agency, Organization for Economic, Paris, France, 2006.

[7] F. G. Montoya, A. Peña-García, A. Juaidi, and F. Manzano-Agugliaro, "Indoor lighting techniques: An overview of evolution and new trends for energy saving," *Energy Buildings*, vol. 140, pp. 50–60, Apr. 2017.

[8] X. Long et al., "A review on light-emitting diode based automotive headlamps," *Renew. Sustain. Energy Rev.*, vol. 41, pp. 29–41, Jan. 2015.

[9] J. Liang et al., "Far-red-emitting double-perovskite  $\text{CaLaMgSbO}_6:\text{Mn}^{4+}$  phosphors with high photoluminescence efficiency and thermal stability for indoor plant cultivation LEDs," *RSC Adv.*, vol. 8, no. 55, pp. 31666–31672, 2018.

[10] N. G. Yeh, C.-H. Wu, and T. C. Cheng, "Light-emitting diodes—Their potential in biomedical applications," *Renew. Sustain. Energy Rev.*, vol. 14, no. 8, pp. 2161–2166, Oct. 2010.

[11] I. Chew, D. Karunatilaka, C. P. Tan, and V. Kalavally, "Smart lighting: The way forward? Reviewing the past to shape the future," *Energy Buildings*, vol. 149, pp. 180–191, Aug. 2017.

[12] Y. Wang, Y. Wang, N. Chi, J. Yu, and H. Shang, "Demonstration of 575-Mb/s downlink and 225-Mb/s uplink bi-directional SCM-WDM visible light communication using RGB LED and phosphor-based LED," *Opt. Express*, vol. 21, no. 1, pp. 1203–1208, 2013.

[13] M. Meneghini, L.-R. Trevisanello, G. Meneghesso, and E. Zanoni, "A review on the reliability of GaN-based LEDs," *IEEE Trans. Device Mater. Rel.*, vol. 8, no. 2, pp. 323–331, Jun. 2008.

[14] B. Sun, X. Jiang, K. Yung, J. Fan, and M. G. Pecht, "A review of prognostic techniques for high-power white LEDs," *IEEE Trans. Power Electron.*, vol. 32, no. 8, pp. 633–636, Aug. 2017.

[15] A. A. Efremov et al., "Effect of the joule heating on the quantum efficiency and choice of thermal conditions for high-power blue InGaN/GaN LEDs," *Semiconductors*, vol. 40, no. 5, pp. 605–610, May 2006.

[16] J. Park and C. C. Lee, "An electrical model with junction temperature for light-emitting diodes and the impact on conversion efficiency," *IEEE Electron Device Lett.*, vol. 26, no. 5, pp. 308–310, May 2005.

[17] M. Arik, J. Petroski, and S. Weaver, "Thermal challenges in the future generation solid state lighting applications: Light emitting diodes," in *Proc. 8th Intersoc. Conf. Therm. Thermomech. Phenomena Electron. Syst.*, May/June 2002, pp. 113–120.

[18] N. Trivellini, M. Meneghini, M. Buffolo, G. Meneghesso, and E. Zanoni, "Failures of LEDs in real-world applications: A review," *IEEE Trans. Device Mater. Rel.*, vol. 18, no. 3, pp. 391–396, Sep. 2018.

[19] I. E. Titkov et al., "Temperature-dependent internal quantum efficiency of blue high-brightness light-emitting diodes," *IEEE J. Quantum Electron.*, vol. 50, no. 11, pp. 911–920, Nov. 2014.

[20] I. A. Sukhoivanov, O. V. Mashoshyna, V. K. Kononenko, and D. V. Ushakov, "Temperature dependence of the threshold and Auger recombination in asymmetric quantum-well heterolasers," *Proc. SPIE*, vol. 5582, pp. 203–210, Sep. 2004.

[21] Y. C. Shen, G. O. Mueller, S. Watanabe, N. F. Gardner, A. Munkholm, and M. R. Krames, "Auger recombination in InGaN measured by photoluminescence," *Appl. Phys. Lett.*, vol. 91, no. 14, Aug. 2007, Art. no. 141101.

[22] J. Iveland, L. Martinelli, J. Peretti, J. S. Speck, and C. Weisbuch, "Direct measurement of Auger electrons emitted from a semiconductor light-emitting diode under electrical injection: Identification of the dominant mechanism for efficiency droop," *Phys. Rev. Lett.*, vol. 110, no. 17, 2013, Art. no. 177406.

[23] X. A. Cao, E. B. Stokes, P. M. Sandvik, S. F. LeBoeuf, J. Kretschmer, and D. Walker, "Diffusion and tunneling currents in GaN/InGaN multiple quantum well light-emitting diodes," *IEEE Electron Device Lett.*, vol. 23, no. 9, pp. 535–537, Sep. 2002.

[24] S. Karpov, "ABC-model for interpretation of internal quantum efficiency and its droop in III-nitride LEDs," in *Proc. Numer. Simulation Optoelectron. Devices*, Sep. 2014, pp. 1293–1303.



- [25] R. Vaxenburg, A. Rodina, E. Lifshitz, and A. L. Efros, "The role of polarization fields in Auger-induced efficiency droop in nitride-based light-emitting diodes," *Appl. Phys. Lett.*, vol. 103, Nov. 2013, Art. no. 221111.
- [26] J. Piprek, "Efficiency droop in nitride-based light-emitting diodes," *Phys. Status Solidi A*, vol. 207, no. 10, pp. 2217–2225, 2010.
- [27] C.-C. Pan et al., "Reduction in thermal droop using thick single-quantum-well structure in semipolar (2021) blue light-emitting diodes," *Appl. Phys. Express*, vol. 5, no. 10, 2012, Art. no. 102103.
- [28] Y.-W. Lin, C.-K. Wang, Y.-Z. Chiou, H.-M. Chang, and S.-J. Chang, "Investigation of optical and electrical properties of GaN-based blue light-emitting diodes with various quantum well thicknesses," *Proc. SPIE*, vol. 5, no. 1, Jul. 2015, Art. no. 057612.
- [29] D. F. Feezell, J. S. Speck, S. P. Denbaars, and S. Nakamura, "Semipolar (2021) InGaN/GaN light-emitting diodes for high-efficiency solid-state lighting," *J. Display Technol.*, vol. 9, no. 4, pp. 190–198, Apr. 2013.
- [30] M. F. Schubert et al., "Effect of dislocation density on efficiency droop in GaInN/GaN light-emitting diodes," *Appl. Phys. Lett.*, vol. 91, Nov. 2007, Art. no. 231114.
- [31] B. Monemar and B. E. Sernelius, "Defect related issues in the "current roll-off," in InGaN based light emitting diodes," *Appl. Phys. Lett.*, vol. 91, Oct. 2007, Art. no. 181103.
- [32] M.-H. Kim, "Origin of efficiency droop in GaN-based light-emitting diodes," *Appl. Phys. Lett.*, vol. 91, Sep. 2007, Art. no. 183507.
- [33] C. Yu, J. Fan, C. Qian, X. Fan, and G. Zhang, "Luminous flux modeling for high power LED automotive headlamp module," in *Proc. 18th Int. Conf. Electron. Packag. Technol. (ICEPT)*, Aug. 2017, pp. 1389–1395.
- [34] J. Fan, M. G. Mohamed, C. Qian, X. Fan, G. Zhang, and M. Pecht, "Color shift failure prediction for phosphor-converted white LEDs by modeling features of spectral power distribution with a nonlinear filter approach," *Materials*, vol. 10, no. 7, p. 819, Jul. 2017.
- [35] Y. Xi and E. F. Schubert, "Junction-temperature measurement in GaN ultraviolet light-emitting diodes using diode forward voltage method," *Appl. Phys. Lett.*, vol. 85, no. 12, pp. 2163–2165, 2004.
- [36] X. Luo, X. Fu, F. Chen, and H. Zheng, "Phosphor self-heating in phosphor converted light emitting diode packaging," *Int. J. Heat Mass Transf.*, vol. 58, nos. 1–2, pp. 276–281, 2013.



**WEI CHEN** received the B.S. degree from the Qingdao University of Technology, Qingdao, China, in 2017. He is currently pursuing the master's degree with the College of Mechanical and Electrical Engineering, Hohai University, Changzhou, China. He is also an Intern Student of the Changzhou Institute of Technology Research for Solid State Lighting, Changzhou, China. His main research interests include the thermal management of solid state lighting sources, such as

LED and laser, design of automotive lighting systems, and the reliability assessment and failure mechanism analysis of electronic devices.



**JIAJIE FAN** (S'12–M'14–SM'17) received the B.S. degree in inorganic materials science and engineering from the Nanjing University of Technology, Nanjing, China, in 2006, the M.S. degree in material science and engineering from the East China University of Science and Technology, Shanghai, China, in 2009, and the Ph.D. degree in industrial and systems engineering from The Hong Kong Polytechnic University, Hung Hom, Hong Kong, in 2014. He is currently an Associate

Professor with the College of Mechanical and Electrical Engineering, Hohai University, Changzhou, Jiangsu, China. He is also a Postdoctoral Research Fellow with the Beijing Research Centre, Delft University of Technology, and the State Key Laboratory of Solid State Lighting, China. His main research interests include reliability assessment for LEDs, prognostics and health management for LED lightings, failure diagnosis and prognosis for electric devices and systems, and advanced microelectronic packaging and assembly. He is an Associate Editor of the IEEE ACCESS journal and a register of certified Six Sigma Green Belt in Hong Kong Society for Quality (HKSQ).



**CHENG QIAN** (M'16) received the B.S. and M.S. degrees in materials science and technology from the Beijing Institute of Technology, in 2003 and 2006, respectively, and the Ph.D. degree in aerospace engineering from the Delft University of Technology, in 2013. He held a postdoctoral fellowship position with the State Key Laboratory of Solid State Lighting, Institute of Semiconductors, Chinese Academy of Science. He was a Program Manager with the Changzhou

Institute of Technology Research for Solid State Lighting, China. He is currently an Associate Professor with Beihang University. His main research interests include reliability modeling, and design optimization of complicated electronic devices using combined knowledge of multi-physics numerical simulations and statistical theories.



**BIN PU** received the M.S. degree in software engineering from Tongji University, Shanghai, China, in 2004. He is currently a Project Manager with the Changzhou Institute of Technology Research for Solid State Lighting, China. His main research interests include software engineering and the Internet of Things.



**XUEJUN FAN** (SM'06–F'19) received the Ph.D. degree in solid mechanics from Tsinghua University, Beijing, China, in 1989. He is currently a Professor with the Department of Mechanical Engineering, Lamar University, Beaumont, TX, USA. He has published over 250 technical papers, four books, 25 book chapters, and several patents. His research interests include multi-physics and multi-scale modeling, and characterization for heterogeneous system materials and packaging.

He holds the title of University Professor at Lamar University. He is an IEEE Distinguished Lecturer. He received the Outstanding Sustained Technical Contribution Award, in 2017, and Exceptional Technical Achievement Award from the IEEE Electronic Packaging Society, in 2011. In his earlier career, he was promoted to a Full Professor at the age 27 with the Taiyuan University of Technology, Shanxi, China, in 1991, and became one of the youngest Full Professors in China.



**GUOQI ZHANG** (M'03–F'14) received the Ph.D. degree in aerospace engineering from the Delft University of Technology, Delft, The Netherlands, in 1993. Since 2013, he has been a Chair Professor with the Department of Microelectronics, Delft University of Technology. He had been with Philips for 20 years, as a Principal Scientist, from 1994 to 1996, a Technology Domain Manager, from 1996 to 2005, a Senior Director of Technology Strategy, from 2005 to 2009, and

a Philips Fellow, from 2009 to 2013. He also had part time appointments as a Professor with the Technical University of Eindhoven, from 2002 to 2005, and as a Chair Professor with the Delft University of Technology, from 2005 to 2013. He is one of the pioneers in developing the More than Moore (MtM) strategy when he served as a Chair of MtM Technology Team of European's Nanoelectronics Platform, in 2005. He has published more than 400 papers, including more than 150 journal papers, three books, 17 book chapters, and more than 100 patents. His research interests include heterogeneous micro/nanoelectronics packaging, system integration, and reliability. He received the Outstanding Contributions to Reliability Research Award from the European Center for Micro/Nanoreliability, in 2007, the Excellent Leadership Award from EuroSimE, the Special Achievement Award from ICEPT, and the IEEE Components, Packaging, and Manufacturing Technology Society Outstanding Sustained.

• • •